WILEY-VCH

DOI: 10.1002/
Full Paper

Fragile-to-Strong Crossover in Supercooled Liquid Ag-In-Sb-Te Studied by Ultrafast Calorimetry

*Jiri Orava, Daniel W. Hewak, and A. Lindsay Greer**

Dr. J. Orava, Prof. A. L. Greer
Department of Materials Science & Metallurgy, 27 Charles Babbage Road, Cambridge CB3 0FS, United Kingdom
E-mail: alg13@cam.ac.uk

Dr. J. Orava, Prof. A. L. Greer
WPI Advanced Institute for Materials Research, Tohoku University, 2-1-1 Katahira, Aoba-ku, Sendai 980-8577, Japan

Prof. D. W. Hewak
Optoelectronics Research Centre, University of Southampton, Southampton SO17 1BJ, United Kingdom

Keywords: phase-change memory, chalcogenide glasses, crystallization, fragile-to-strong crossover, ultrafast calorimetry

Phase-change random-access memory relies on the reversible crystalline-glassy phase change in chalcogenide thin films. In this application, the speed of crystallization is critical for device performance: there is a need to combine ultrafast crystallization for switching at high temperature with high resistance to crystallization for non-volatile data retention near to room temperature. In phase-change media such as *nucleation-dominated* $Ge_2Sb_2Te_5$, these conflicting requirements are met through the highly 'fragile' nature of the temperature dependence of the viscosity of the supercooled liquid. The present study explores, using ultrafast-heating calorimetry, the equivalent temperature dependence for the *growth-dominated* medium Ag-In-Sb-Te. The crystallization shows (unexpectedly) Arrhenius temperature dependence over a wide intermediate temperature range. Here it is shown that this is evidence for a *fragile-to-strong crossover* on cooling the liquid. Such a crossover has many consequences for the

interpretation and control of phase-change kinetics in chalcogenide media, helping to understand the distinction between nucleation- and growth-dominated crystallization, and offering a route to designing improved device performance.

1. Introduction

In chalcogenide-based phase-change memory (PCM), Joule heating by weaker or stronger electrical pulses gives, respectively, crystallization, or melting and subsequent revitrification, of a memory cell. Because a cell can be put into intermediate states (of partial crystallinity), such switching is of great interest not only for non-volatile memory,[1] but also potentially for neuromorphic computing in which progressive transformation mimics the operation of biological synapses.[2] The kinetics of switching needs to be better understood for optimization of phase-change (PC) materials and devices. Critically, crystallization must be rapid, preferably taking less than the 10 ns switching time typical for DRAM.[3,4] In the application of chalcogenides in optical discs (CD-RW, DVD-RW etc.), where heating is by laser pulses, two patterns of crystallization have been distinguished: in *growth-dominated* materials, e.g. (Ag,In)-doped Sb_2Te (Ag-In-Sb-Te, AIST), a glassy mark in the crystalline film transforms by growth of crystals inward from its perimeter; in *nucleation-dominated* materials, e.g. $Ge_2Sb_2Te_5$ (GST), crystals nucleate and grow within the mark.[5,6] The present kinetic study allows us to explore further the origin of the distinction between the two types of PC material, and the relevance of the distinction for PCM.

For chalcogenides of interest for PCM, there have been many studies of the kinetics of crystal nucleation and growth near to the glass-transition temperature T_g, but only recently have measurements been made over the much wider temperature range, up to the maximum in crystal growth rate, relevant for understanding PCM operation. For GST, Orava et al.[7] used

ultrafast differential scanning calorimetry (DSC) to estimate the crystal growth rate *U* nearly up to its maximum: the temperature dependence of *U* is markedly non-Arrhenius, associated with the viscosity η in a liquid that is *fragile* in the Angell classification.[8] Later work by others, modeling polycrystalline microstructure development[9] and direct electrical measurements of PCM cells,[10,11] has suggested the same general form of $U(T)$ in GST, with the maximum in *U* being around $0.76T_{\mathrm{m}}$ (T_{m} : melting temperature). Crystallization in PC materials is now accepted to be non-Arrhenius.[12] Orava et al.[7] also noted evidence for a decoupling of *U* from η on cooling to near T_{g}. Such decoupling, surveyed for a variety of glass-forming systems by Ediger et al.,[13] is associated with a breakdown in the Stokes-Einstein relationship between atomic diffusivity and η, and is greater for more fragile systems. With decoupling, *U* is faster than would be estimated from a simple inverse proportionality to η. Decoupling can be expected in chalcogenides such as GST and TeGe because their liquids are fragile, and it has been studied, for example, by molecular dynamics (MD).[14]

Salinga et al.[15] used time-resolved laser reflectometry to make isothermal measurements of *U* in AIST in the range 418 to 553 K. The values of *U* span 8 orders of magnitude, from 1×10^{-7} to >3 m s^{-1}, and over the entire range are close to an Arrhenius temperature dependence, unlike GST. Again unlike GST, there is no evidence for decoupling of *U* and η; furthermore, using the degree of decoupling as an adjustable parameter does not help in fitting models for *U* in the supercooled liquid to measured values (Suppl. Info of Ref. [15]).

As Salinga et al. note, the Arrhenius dependence of *U* cannot continue up to T_{m} ; at higher temperatures than their measurements "a quite dramatic change in the temperature dependence of the crystal growth velocity must occur".[15] In the present work, we apply ultrafast DSC as in Ref. [7] to AIST. The unexpected Arrhenius regime is confirmed, over a wide temperature range. We suggest that this does not indicate an isoconfigurational regime as suggested in Ref. [15], but rather the opposite — a crossover, on cooling, from a *fragile* to

a *strong* liquid. Such a crossover would have profound implications for the modeling and actual operation of PCM.

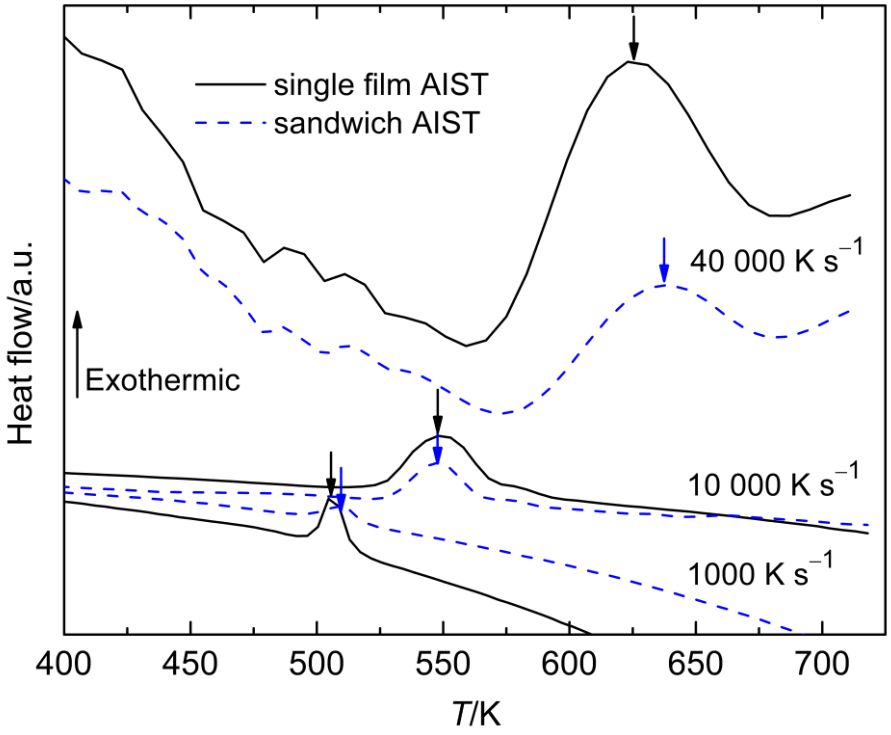

Figure 1. Ultrafast heating of as-deposited amorphous AIST. DSC traces for 270-nm single films (solid lines) and for 60-nm films sandwiched between ZnS:SiO_2 dielectric layers (dashed lines). Each trace, labeled with the corresponding heating rate (Φ), has an exothermic peak (arrowed at peak maximum T_p) indicating crystallization. The values of T_p as a function of Φ allow the activation energy for crystallization to be determined by the Kissinger method[16] (Figure 2).

2. Results

2.1. Kissinger Analysis of Crystallization

Conventional (near T_g) studies of PC thin films show that crystallization kinetics can be altered by the addition of capping or sandwiching layers. The studies of Salinga et al. were on AIST sandwiched between ZnS:SiO_2 layers.[15] In thin-film resistometry of AIST up to ~ 440 K , Njoroge et al.[17] found that a capping layer of ZnS:SiO_2 impedes crystallization; the

effect is weak, but greater at higher temperature, characterized as a decrease in the activation energy of crystallization from 3.03 eV to 2.39 eV. In the present study, it is therefore of interest to compare AIST thin films when free-standing and when sandwiched between ZnS:SiO_2 layers. Ultrafast DSC traces of as-prepared films in both states (**Figure 1**) show crystallization exotherms with peak temperatures T_p increasing from ~480 K to ~630 K as the heating rate Φ is increased from $50\,\mathrm{K\,s^{-1}}$ to $40\,000\,\mathrm{K\,s^{-1}}$. The crystallization rate can thus be studied to higher temperature than has been possible with other methods.

The data from ultrafast DSC and published data from conventional measurements at lower Φ are combined in **Figure 2**. In this Kissinger plot, the gradient of the line is $-Q/R$ (Q: activation energy of crystallization; R: gas constant). As discussed earlier,[7,16] the activation energy can be taken as that for crystal growth. The ultrafast DSC data provide a natural extension of the conventional measurements. At lower Φ in the ultrafast data, up to $T_p \approx 550\,\mathrm{K}$, the exotherms for the sandwiched film have somewhat higher T_p than for the single film, reflecting an impeding effect. However, this effect is not as large as would be expected from an extrapolation of the conventional-heating-rate data of Njoroge et al.[17] (inset, Figure 2). At higher Φ, $T_p > 550\,\mathrm{K}$, the values of T_p show exceptionally wide scatter, and the values in the single film are now higher, similar to the effect seen in the comparison of single and sandwiched films of GST.[18] Unlike GST, however, the data points in Figure 2 appear to fall on a curve showing a maximum (at ~620 K). The spread in T_p values and the maximum in the Kissinger curve may arise from the difficulty of crystal nucleation in growth-dominated AIST, a difficulty somewhat lessened in the sandwiched film. These results also suggest that at even higher Φ, much beyond the range of the present ultrafast DSC, amorphous/glassy AIST would transform directly into the liquid, avoiding crystallization.

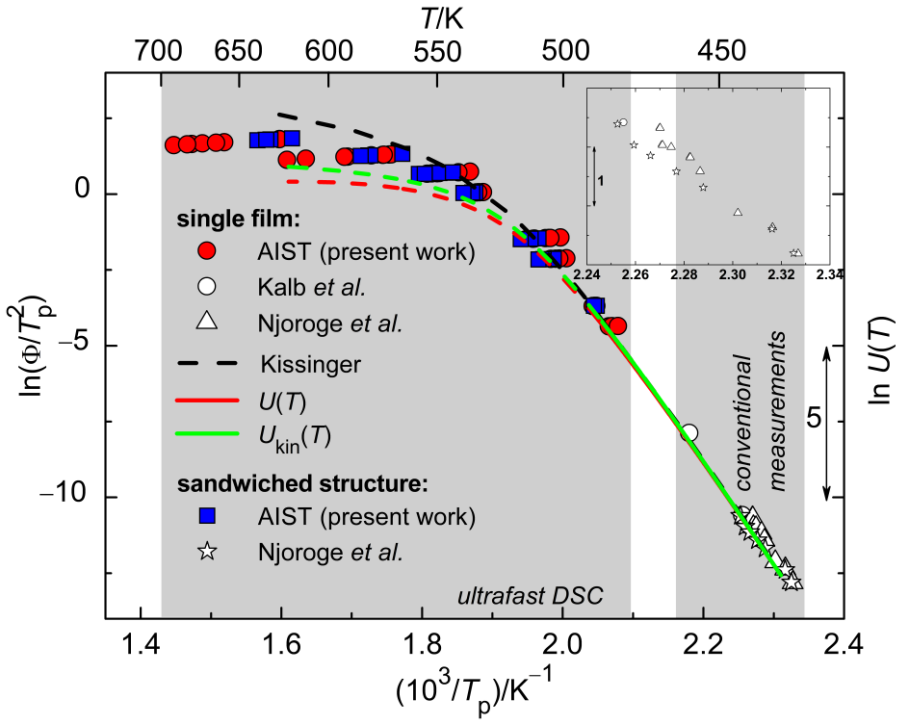

Figure 2. Kissinger plot for crystallization of supercooled liquid AIST. The exotherm peak temperature T_p in DSC, or an equivalent point for crystallization on heating in a different technique, increases with heating rate Φ. In this plot, the gradient is $-Q/R$, where Q is the activation energy of crystallization, to a good approximation that for crystal growth.[7,16] The solid data points are from the present work on ultrafast DSC (example traces in Figure 1). The data of Kalb et al.[19] are from conventional DSC ($Ag_{5.5}In_{6.5}Sb_{59}Te_{29}$, 7 μm-thick films), Φ = 0.083 and 1.3 K s^{-1}. The data of Njoroge et al.[17] ($Ag_5In_6Sb_{59}Te_{30}$ single 100 nm films and capped AIST(100 nm)/ZnS:SiO_2(5 nm)) are from resistometry, $\Phi = 4.5\times10^{-3}$–5.7×10^{-2} K s^{-1}. The lines come from modeling as in Ref. [16] to achieve a Kissinger best-fit (left-hand abscissa) to measured T_p. The kinetic coefficient for crystal growth U_{kin} (right-hand abscissa) is the parameter of fundamental interest, scaling inversely with the liquid viscosity. The shaded bands show the range of T_p observable by conventional and ultrafast heating. The inset shows a close-up of the low-temperature data.

2.2. Temperature Dependence of Viscosity

Together, the ultrafast-DSC data and the conventional measurements show Arrhenius behavior over >5 orders of magnitude and, at higher temperature, the dramatic change in the temperature dependence of the kinetics anticipated by Salinga et al.[15] can be seen. Our attempt to fit the data follows the procedures in earlier work[7] as detailed in Section 5. The temperature-dependent viscosity $\eta(T)$ of the supercooled liquid is taken to follow the

extension of the free-growth model developed by Cohen and Grest,[20] and described by their expression

$$\log_{10}\eta = A - \frac{2B}{T - T_0 + \left[(T - T_0)^2 + 4CT\right]^{1/2}}\ , \tag{1}$$

with *A*, *B*, *C* and T_0 being adjustable parameters. The kinetic coefficient for crystal growth, U_{kin}, is taken to be inversely proportional to η. Assuming continuous normal growth (as in Ref. [13]), the crystal growth rate *U* is given by

$$U = U_{\text{kin}}\left[1 - \exp\left(-\frac{\Delta G}{RT}\right)\right], \tag{2}$$

where ΔG (a positive quantity) is the thermodynamic driving force for crystallization. We estimate the temperature-dependent ΔG using the expression of Thompson and Spaepen[21]

$$\Delta G(T) = \frac{\Delta H_{\text{m}}\Delta T}{T_{\text{m}}}\left(\frac{2T}{T_{\text{m}} + T}\right), \tag{3}$$

where ΔT is the supercooling. We take the latent heat of melting $\Delta H_{\text{m}} = 16.1\,\text{kJ mol}^{-1}$ and the melting temperature $T_{\text{m}} = 810\,\text{K}$ (from Ref. [19]). The temperature-dependent *U* is then used in numerical modeling[16] of the crystallization on heating to simulate DSC traces; this simulation is necessary as the *Q* given directly by the Kissinger plot deviates from that for *U* at high Φ.

The parameters in Equation (1) are adjusted to fit the measured Kissinger plot. In the previous work on GST, this was found to be straightforward.[7] In the present work on AIST, however, the best fit that could be obtained (dashed line in Figure 2) fails at high Φ. One factor is that Equation (1), though it can match the data for many systems,[20] appears not to be able to fit the sharp change in the temperature dependence found for AIST. A second, more important, factor is that the maximum in the Kissinger data (in Figure 2, noted above) is incompatible with the numerical model[16] used to simulate the DSC exotherms. The model has been tested for a variety of materials parameters, but never predicts such a levelling-off or maximum. We conclude that for AIST at high heating rates ($\Phi > 200\,\mathrm{K\,s^{-1}}$, $T_\mathrm{p} > 490\,\mathrm{K}$) the model is not applicable and therefore the Kissinger data cannot be applied reliably to extract the temperature dependences of U and U_kin. Accordingly, the fitting to obtain U_kin is applied only at lower Φ, as indicated by the solid (not dashed) green line in Figure 2.

The temperature-dependence of kinetics in AIST is explored further in an Angell plot (**Figure 3**), extended to include the glassy state just below T_g. To construct this, we take T_g (AIST) = 378 K, 5 K lower than for GST (Section 5). We start by collecting published data on $\eta(T)$ for AIST. The viscosity can be measured directly (including from creep or stress relaxation measurements) or can be inferred from $U_\mathrm{kin}(T)$ (for details, see Section 5). Stress-relaxation measurements in the glass give the data shown for $T_\mathrm{g}/T > 1$, which show an activation energy of 1.33 eV.[22] At higher temperatures, Kalb et al.[6] made isothermal measurements of $U(T)$ using atomic force microscopy (AFM) to image the crystals. These data, plotted in terms of $\eta(T)$ on Figure 3, have an activation energy of 2.90 eV.

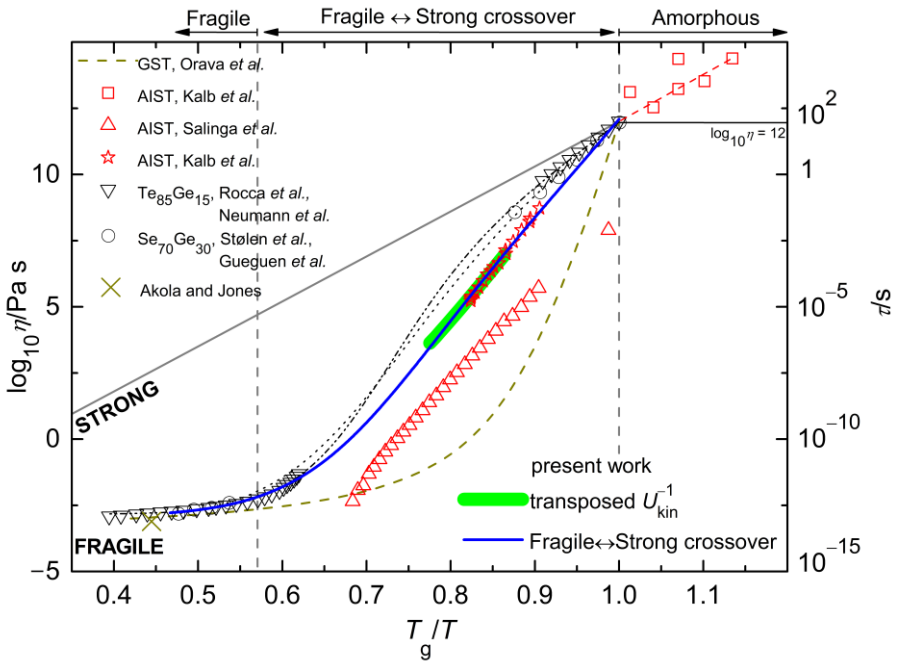

Figure 3. Angell plot for temperature dependence of viscosity. The curve for GST, from Orava et al.,[7] shows the form of $\eta(T)$ expected for a supercooled liquid of a single, high fragility (m = 90). The other data shown do not fit such a form and are interpreted in terms of a fragile-to-strong crossover on cooling the liquid. For AIST, the blue line shows a generalized-MYEGA[23] fit to data in the crossover region derived from AFM-based growth-rate measurements by Kalb et al.[6] on single-film $Ag_{5.5}In_{6.5}Sb_{59}Te_{27}$ (30 nm) and from U_{kin} data (green line) transposed from Figure 2, and to the value for η at 850 K derived from diffusivities in $Ag_{3.5}In_{3.8}Sb_{75.0}Te_{17.7}$ calculated by Akola and Jones.[24] Further AIST data are those derived from reflectometry measurements by Salinga et al.[15] on sandwiched $Ag_4In_3Sb_{67}Te_{26}$ (substrate/SiN (50 nm)/ZnS:SiO_2(10 nm)/AIST(30 nm)/ZnS:SiO_2(100 nm)). All these data in the crossover region show, as expected for a supercooled liquid, a stronger temperature dependence of η than in the amorphous or glassy state (at $T_g/T > 1$ showing data of Kalb et al.[22]). The data for $Te_{85}Ge_{15}$ are from viscosity measurements by Neumann et al.[25] and from a Kissinger analysis of conventional DSC measurements (Φ = 0.083–1.3 K s^{-1}) by Rocca et al.[26] The data for $Se_{70}Ge_{30}$ are from viscosity values collected by Stølen et al.[27] and indentation creep measurements by Gueguen et al.[28] The dashed lines show generalized-MYEGA fits to $\eta(T)$ for these two systems, each showing a clear fragile-to-strong crossover, which the $\eta(T)$ for AIST resembles.

Kissinger-type data such as those in Figure 2 give the temperature dependence, but not the absolute values, of U_{kin}.[7] Given that U_{kin} is inversely proportional to η, the (solid) green line on Figure 2 can be transposed to Figure 3, if given a reference point to fix the absolute values. In previous work,[7] the reference point was η at T_m. This is not possible in the present work because of the lack of fitting for $T_p > 490\,K$ in Figure 2. Instead, we adjust the

absolute value to match the AFM data of Kalb et al;[6] in this way the green line in Figure 3 is obtained, extending the published data to higher temperature. The activation energy for the data transposed from Figure 2 is 2.86 eV, effectively matching that of the AFM data, which are also from as-deposited films. Together, the data from Figure 2 (ultrafast DSC in the present work and conventional resistometry[17] and DSC[19]) and the AFM[6] data suggest an Arrhenius temperature dependence over at least 5 orders of magnitude in $\eta(T)$.

The $U(T)$ obtained in the reflectometry measurements of Salinga et al.[15] gives an Arrhenius $\eta(T)$ extending over an even wider range, of 8 orders (>10 orders if a data point from in-situ electron microscopy is included). The activation energy for the reflectometry data, from melt-quenched films, is 2.70 eV, roughly in agreement with the values already quoted.

3. Discussion

3.1. Arrhenius Behavior

How is the Arrhenius temperature dependence to be understood? Salinga et al.[15] suggest that it represents an isoconfigurational (glassy) state. Their reflectivity measurements[15] are on samples immediately after a quench, as fast as $10^{10}\ \mathrm{K\,s^{-1}}$, from above T_m. During such a rapid quench, the glass transition would be displaced to higher temperature, and if $T_\mathrm{g} \approx 550\,\mathrm{K}$ (i.e. $T_\mathrm{g}/T \approx 0.69$ as plotted in Figure 3) then their data would indeed represent a isoconfigurational tangent to the $\eta(T)$ for the supercooled liquid. This T_g value is, though, very much higher than values inferred from conventional DSC.[6,29]

The AFM data of Kalb et al.,[6] reinforced and extended by the data from Figure 2, show very similar Arrhenius behavior, but are obtained from crystal-growth studies on as-deposited amorphous films. These films have not been subjected to an ultrafast quench, and therefore

are not in the high-energy (high fictive temperature) state associated with an exceptionally high T_g during quenching. Importantly, the similar activation energies for all the Arrhenius data sets are more than twice that of 1.33 eV for the isoconfigurational viscosity in the glass.[22] As noted by Kalb et al.,[6] an activation energy so much higher than that for the isoconfigurational viscosity implies that the crystal growth is in the supercooled liquid (not glassy) state. The lack of time-dependence in the growth rates measured by Kalb et al.,[6] also suggests that the Arrhenius growth is in the liquid state.

The T_g value assumed to apply during the rapid quench in the work of Salinga et al.[15] (~550 K) is >170 K higher than the value used in plotting Figure 3, reflecting continuing uncertainty over the glass transition in PC materials. However, the different values merely place T_g at different points relative to the shape of the data in Figure 3. At T_g the data should show a marked change of slope (higher in the liquid, lower in the glass). Such a change is seen in the AIST data as plotted in Figure 3, consistent with T_g having roughly the value assumed in the present work.

Ab-initio molecular-dynamics (MD) simulations of atomic diffusivity *D* in AIST suggest that there may be a high-temperature regime in which the temperature dependence is weak.[30] Below 550 K, however, exactly when needed for understanding the Arrhenius $U(T)$, the values of *D* given by the MD simulations are higher than those inferred from *U*, and the values diverge further at lower temperature. Zhang et al.[30] attribute this divergence (seen clearly in Figure 3a in their paper) to the different quench rates at which the glasses are formed: ~10^{10} K s^{-1} for experiments determining *U*, ~10^{13} K s^{-1} for the simulations. However, if the two sets of *D* values represent different glassy (isoconfigurational) states, the low-temperature values should lie on parallel, not divergent, Arrhenius lines. In contrast, the observed divergence is just as expected if the growth measurements are in the supercooled

liquid, while the MD simulations are for a glass formed at ~550 K. We explore another possible reason for the divergence in §3.2.

Overall, then, we conclude that the AIST data shown in Figure 3 for $T_g/T < 1$ relate to the liquid state. These data lie between the strong and fragile limits of the Angell plot, but clearly are of a shape that cannot be fitted to a single fragility. The AFM data[6] and the data from Figure 2 indicate moderate fragility ($m \approx 37$, where $m = \left[\mathrm{d}(\log_{10}\eta)/\mathrm{d}(T_g/T)\right]_{T=T_g}$), but this cannot describe the form of $\eta(T)$ at higher temperature close to T_m. We suggest that the data are consistent with a crossover from a *fragile* liquid to a *strong* liquid on cooling; the Arrhenius behavior is then a signature of this crossover and does not imply a single simply activated process.

3.2. A Fragile-to-Strong Crossover in Liquid AIST

The concept of a *fragile-to-strong crossover* was first proposed for water[31] and later for liquid SiO_2[32] where it was suggested that all 'strong' liquids arise as a result of such a crossover, which may be associated with distinct structures and a liquid-liquid phase transition. For chalcogenides, calorimetric transitions have been detected in both equilibrium (above T_m) and supercooled liquids, e.g. in $Te_{85}Ge_{15}$[33] and $Te_{80}Ge_{20-x}Pb_x$.[34] It is suggested these are transitions between high-temperature metallic and low-temperature semiconducting liquids, and $Te_{85}Ge_{15}$, for example, shows a very sharp increase in resistivity on cooling.[25] Fragility crossovers have been found in the chalcogenide Se-Ge[27] and in several metallic-glass-forming liquids,[23,35] and in the latter case the associated structural changes have also been examined.[36] Transitions may also occur below T_g (*polyamorphism*). The transitions in liquid and amorphous phases, now known for many systems, are closely associated with

changes induced under pressure,[37] as has been shown, e.g., for the PC material $Ge_1Sb_2Te_4$.[38] Related polyamorphic switching can also be induced by light.[39]

In Figure 3, data are also shown for $Te_{85}Ge_{15}$ at high[25] and low[26] temperatures, and for $Se_{70}Ge_{30}$ at high[27] and low[28] temperatures. The high-temperature data are from direct measurements of $\eta(T)$; the low-temperature data for $Se_{70}Ge_{30}$ are from measurements of indentation creep;[28] the low-temperature data for $Te_{85}Ge_{15}$ have a temperature dependence (see §5 for discussion of fragility) derived from Kissinger plots of the primary crystallization exotherms in DSC, with absolute value adjusted to give $\eta = 10^{12}$ Pa s at T_g. All these data indicate a fragile-to-strong crossover, with an overall $\eta(T)$ similar to that for AIST. In fitting the fragile-to-strong crossover in $\eta(T)$ of metallic-glass-forming systems, the generalized-MYEGA equation

$$\log\eta = \log\eta_\infty + \frac{1}{T\left[W_1 \exp\left(\frac{-C_1}{T}\right) + W_2 \exp\left(\frac{-C_2}{T}\right)\right]} \tag{4}$$

has been found useful.[23] The two black dashed lines in Figure 3 show fits of Equation (4) to the high- and low-temperature data for $Te_{85}Ge_{15}$ and $Se_{70}Ge_{30}$.[25–28] These provide a good description of the varying fragility, and are quite different in shape from the dashed line that shows the $\eta(T)$ for GST[7] (i.e. without any apparent fragile-to-strong crossover).

For AIST, we similarly apply Equation (4) to the AFM data,[6] the data transposed from Figure 2 (green line in Figure 3) and to the value of η derived from an average of the high-temperature diffusivities calculated by Akola and Jones.[24] The resulting fit (blue line in Figure 3) shows an extensive region of effectively Arrhenius behavior. This is without a clear point of inflection, though such a point is usual for a fragile-to-strong crossover and is seen in the curves for $Te_{85}Ge_{15}$ and $Se_{70}Ge_{30}$.

The reflectometry data of Salinga et al.[15] are displaced relative to the blue line. As noted by Jeyasingh et al. for GST,[11] samples of different origin show kinetics that are quantitatively different, but qualitatively similar in their temperature dependence. This may be the case in comparing AIST in the as-deposited state (blue line) and after a rapid quench from the melt (data of Salinga et al.[15]).

It may also be relevant that a fragile-to-strong crossover, though reversible on cooling and heating, can show *hysteresis*, occurring at lower temperatures on cooling than on heating. Hysteresis has been observed for a Zr-based metallic-glass-forming melt,[40] and there are indications that such effects can be particularly strong in chalcogenide systems such as Te.[41] Hysteretic effects may underlie the displacement of the data of Salinga et al.[15] from the blue line in Figure 3. The data can be viewed as displaced laterally by ~0.075 on the T_g/T scale. The displacement to lower temperatures is as expected for the high cooling rate in the experiments of Salinga et al.[15] The structural relaxation effects seen in the $U(T)$ data from these reflectometry experiments can be regarded as reversion to states of higher η (i.e. towards the blue line on Figure 3). At the even higher effective cooling rates in the MD simulations by Zhang et al.[30], the fragile-to-strong crossover may be displaced to even lower temperature. In that case, the simulations down to 450 K are entirely in the fragile regime, and this provides an alternative explanation for the divergence, already discussed in §3.1, between the diffusivity values from the simulations and those inferred from the growth rate measurements.

3.3. Nucleation- and Growth-Dominated Crystallization

Though the effects of liquid fragility on crystal-growth kinetics have been studied for a wide range of glass-forming systems,[42] the effects of a fragile-to-strong crossover have not so far

been considered. The consequences of such a crossover in PC liquids are explored by examining the form of $U(T)$ (calculated from Equation (2), and taking $\eta(T)$ as given by the blue line in Figure 3) for AIST (**Figure 4**), and comparing with that for GST (from Ref. [7]). In the ideal operation of a PCM cell, crystallization would occur close to the maximum of $U(T)$. For AIST the maximum is estimated to be at $T/T_m = 0.89$, $T_g/T = 0.52$, i.e. in the liquid that is firmly in the high-temperature fragile regime of low viscosity and high mobility, giving high U and short switching times. Thus the fragile-to-strong crossover on cooling is helpful in giving a clear transition between this regime of fast switching and a regime of low mobility for data retention. The contradictory needs for switching and retention are a focus for optimization of PC materials.[3]

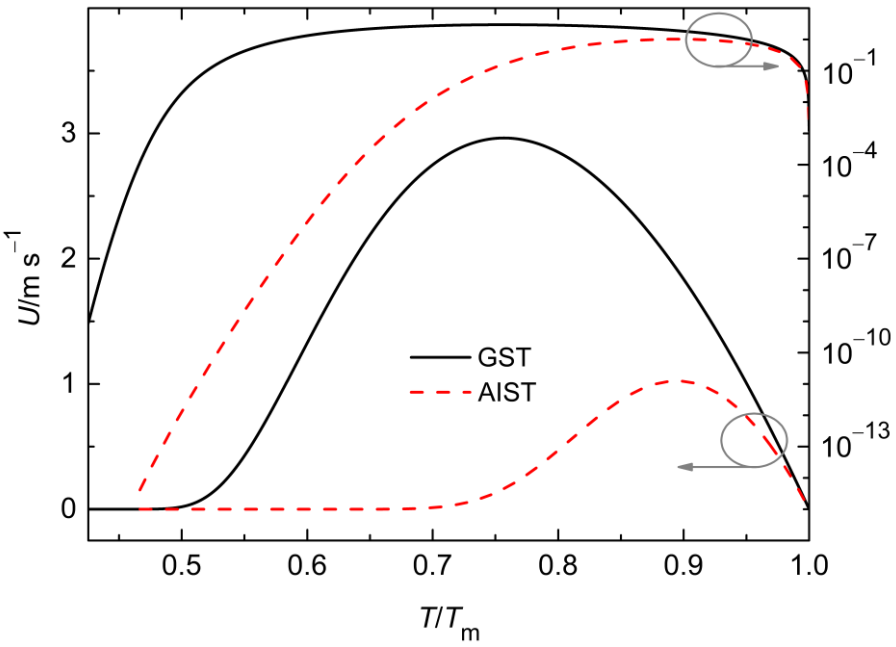

Figure 4. Comparison of crystal growth rates in supercooled liquid AIST and GST from T_g to T_m. The growth rate $U(T)$ in AIST is compared with earlier data for GST.[7] The $U(T)$ for GST is calculated from a Cohen-Grest[20] fit to $\eta(T)$ for a liquid of fragility m = 90, and with a decoupling parameter of ξ = 0.67 (i.e. $U \propto \eta^{-0.67}$). The $U(T)$ for AIST is calculated from a generalized-MYEGA[23] fit (blue line) to the data in Figure 3, representing a fragile-to-strong crossover on cooling. The logarithmic plots (right-hand abscissa) show that the maximum growth rates in the two systems are similar, relevant for fast PCM switching. Below 0.7 T_m, the kinetics in AIST become much slower than in GST, hindering homogeneous nucleation of crystals which has its maximum rate at ~0.6 T_m. This may contribute to AIST showing *growth-dominated* crystallization.

Figure 4 suggests that although the maximum values of $U(T)$ are broadly similar for AIST and GST, the temperature of the maximum is displaced to a higher relative value for AIST. At temperatures below the maxima in $U(T)$, the growth rates, dominated by U_{kin} and so simply inversely proportional to $\eta(T)$, diverge strongly. The maximum in the rate of homogeneous nucleation of crystals occurs at a lower temperature than the maximum in $U(T)$, because of the nucleation barrier arising from the interfacial energy between crystal and liquid; the maximum is typically at $T/T_{\text{m}} \approx 0.6$.[43,44] For AIST this corresponds to $T_{\text{g}}/T \approx 0.8$, well within the crossover range. At this T/T_{m} the η is thus much higher for AIST than for GST. Based only on the relative kinetics at $T/T_{\text{m}} \approx 0.6$ in Figure 4, we can estimate that, in the absence of other factors (e.g. differing crystal-liquid interfacial energy), the maximum nucleation rate for AIST would be lower (by 6 orders of magnitude) than for GST. The key point is that the distinctive shape of $\eta(T)$ when there is a fragile-to-strong crossover in a suitable temperature range is to increase, possibly dramatically, the ratio of the maximum growth rate to the maximum nucleation rate. Thus the existence of a fragile-to-strong crossover may explain why crystallization in AIST is growth-dominated (nucleation is suppressed in the strong liquid) while in GST it is nucleation-dominated. The relative suppression of nucleation in AIST may be relevant in different ways, on heating or isothermal annealing of an as-deposited film (in ultrafast DSC or in conventional measurements[17,19,45]) or in generating quenched-in nuclei on cooling (as in Ref. [15]). The importance of quenched-in nuclei in the contrasting crystallization behavior of AIST and GST has been studied using fluctuation transmission electron microscopy.[46]

3.4. Decoupling of Growth and Viscous Flow

In the analysis of crystal-growth kinetics in single-film GST, Orava et al.[7] found it necessary to assume a progressive decoupling of $U(T)$ from $\eta(T)$ as the temperature is lowered from T_m to T_g. At T_g, U was estimated to be ~5 orders of magnitude faster than it would be if growth remained fully coupled to viscous flow. In the light of the present analysis for AIST, it is pertinent to ask whether this disparity might alternatively be explained by a fragile-to-strong crossover in GST. We cannot rule this out, but the very different shapes of $\eta(T)$ in the two cases suggest that any crossover in GST, if it occurs, is at lower temperature than in AIST, largely obscured by the glass transition. There is currently a lack of data in the most relevant temperature range. Decoupling is expected to be most evident in a fragile liquid at low temperature (just above T_g).[13] We note that there can be little or no role for decoupling in the case of a fragile-to-strong crossover, as the fragile liquid does not persist to low temperature.

4. Conclusions

Ultrafast DSC enables crystallization in the phase-change chalcogenide AIST to be studied to much higher temperatures (nearly $0.8T_m$) than in previous work, and shows that crystal growth has an Arrhenius temperature dependence over a wide temperature range. Together with conventional kinetic data at lower temperatures and by comparison with other chalcogenides, the new data provide evidence for a crossover from fragile to strong liquid behavior on cooling. Such a crossover appears to be widespread in glass-forming liquids,[47] and may be a general feature of chalcogenide PC liquids, the key question being: where does it occur in relation to the key temperatures T_g and T_m? A fragile-to-strong crossover would undoubtedly be helpful for PCM in accelerating switching while improving data retention. As

work, for example, on $Te_{80}Ge_{20-x}Pb_x$[34] has shown, the temperature of liquid-liquid transitions can be tuned by altering the composition. In PC Sb-Ge materials, reduction of Ge content changes $U(T)$ from a non-Arrhenius form typical for a fragile liquid to an Arrhenius form possibly similar in origin to that discussed here.[45] Tuning of the fragility of GST has been achieved by addition of dopants.[48] The concept of tuning the crossover temperature may be important in developing optimized PC materials, and the study of transitions under pressure may assist in this.[27,38] Differing properties of the fragile and strong liquids on either side of the crossover (e.g. changes in resistivity associated with changes in bonding type, as explored for $Te_{85}Ge_{15}$[25]) may also be important in understanding and modeling the operation of PCM. There is a clear need for more studies of the structure and property changes associated with the crossover. Structural relaxation effects seen in melt-spun metallic glasses can be associated with the fragile-to-strong crossover,[36] and it is likely that such effects would be still more evident in chalcogenide glasses, which in PCM are formed at quenching rates > 10^4 times higher than in melt-spinning.

5. Methods Section

Sample Preparation: Amorphous thin films (thickness ~270 nm) of $Ag_{5.5}In_{6.5}Sb_{59}Te_{29}$ (AIST) were deposited onto pre-cleaned glass microscope slides by RF magnetron sputtering in a Nano 38 system (Kurt J. Lesker) with a base pressure of 6×10^{-3} Pa, using targets from Mitsubishi (product no. IAST 27-1266). Deposition was at a power of 55 W with an argon flow rate of 20 cm^3 min^{-1} and pressure held at 0.3 Pa. The target-to-substrate distance of 150 mm gave deposits of low stress. The substrates, initially at room temperature, heated by <10 K during deposition. Sandwich structures were made by depositing 10 nm of $ZnS:SiO_2$ (80:20 mol.%) then 60 nm of AIST and finally a capping layer of 10 nm $ZnS:SiO_2$. The deposition

conditions were the same as for the single AIST films except that the argon flow rate during the sputtering of the dielectric layers was 15 cm^3 min^{-1}. The AIST composition in the present work is the same as that in most of the cited studies;[6,19,22,29] it is very close to the $Ag_5In_6Sb_{59}Te_{30}$ studied by Njoroge et al.[17] and further from the $Ag_{3.5}In_{3.8}Sb_{75.0}Te_{17.7}$ in the molecular-dynamics studies of Akola and Jones.[24]

Ultrafast DSC: Power-compensation differential scanning calorimetry (DSC) was performed using a Mettler-Toledo Flash DSC 1, an instrument based on a thin-film geometry and operating on the principles described by Zhuravlev and Schick.[49] Samples were heated at 50 K s^{-1} to 40 000 K s^{-1} under a nitrogen flow of 20 cm^3 min^{-1}. Temperature calibration was performed, at different heating rates, by measuring the onset of melting of a 1 μg sample of indium; the thermal lag is up to 4 K at 10 000 K s^{-1} (for further details see the Suppl. Info. of Ref. [7]). As-deposited single films and sandwiched structures were peeled off the substrates (previous experience including TEM observation suggests that the sandwich structure remains intact[18]) and masses of less than 100 ng were transferred onto the sample area (an Al plate 0.5 mm in diameter) on the chip sensor. The corresponding reference area is used 'empty' (i.e. with no reference material on top).

Kissinger Analysis and Cohen-Grest Fitting of η(T): Our analysis follows that of Orava et al.[7] Following the arguments set out in the Suppl. Info. of Ref. [7], it is assumed that on heating as-deposited amorphous films, crystal nucleation precedes growth and that the crystallization kinetics can be modeled as occurring from a fixed number of centers. As the crystallization is assumed to be polymorphic (amorphous and crystalline phases having the same composition), the crystal growth rate $U(T)$ is taken to be dependent only on temperature, and not on time or crystal radius. The kinetic analysis and the simulation of DSC peaks to fit the Kissinger plot are detailed in Ref. [16]. This analysis appears to work well for nucleation-

dominated GST, [7] but (as noted in the discussion of Figure 2) it appears to fail at the highest heating rates Φ for growth-dominated AIST.

The liquid viscosity η is assumed to follow Equation (1). This expression, derived from the free-volume theory as extended by Cohen and Grest,[20] shows excellent agreement with experiment, over 12 orders of magnitude in η, for a wide variety of systems. The effective value of the atomic diffusion coefficient *D* is related to η through the Stokes-Einstein relation:

$$D = \frac{kT}{3\pi a \eta}, \tag{5}$$

where *k* is Boltzmann's constant, and *a* is an effective atomic diameter or jump distance, set to be 0.30 nm (from the average interatomic spacing, i.e. bond length, determined by Zhang et al.[30]). For growth that is rate-limited by diffusive processes at the crystal-liquid interface (not by long-range transport of solute or heat) the kinetic coefficient for growth U_{kin} (i.e. the limiting velocity at high driving force) is given by

$$U_{\mathrm{kin}} = \frac{D}{a}. \tag{6}$$

The growth rate *U* is related to U_{kin} through Equation (2). The parameters in Equation (1), adjusted to obtain the fit shown in Figure 2, have the values: B = 20.9±0.9 K, C = 0.70±0.03 K, T_0 = 517±1 K, with the quality of fit given by R^2 = 0.9997. (The value of the fitting parameter *A* is of no direct significance since absolute values of η are not determined.)

Angell Plot and Generalized-MYEGA Fitting of η(T): The plotting of Figure 3 requires a value for the glass-transition temperature T_{g} of AIST. As discussed in detail in the Suppl.

Info. of Ref. [7], the identification of T_g values for PC materials is difficult. We follow the suggestion of Kalb et al.[29] that the T_g of AIST is ~5 K lower than that of GST. Consistent with our assumption that $T_g(\mathrm{GST}) = 383\,\mathrm{K}$,[7] here we take $T_g(\mathrm{AIST}) = 378\,\mathrm{K}$.

The blue line in Figure 3 is a fit to a presumed fragile-to-strong crossover in AIST based on the generalized-MYEGA equation, Equation (4), developed by Zhang et al.[23] This is a modification of the original MYEGA equation[50] based on Adam-Gibbs theory.[51] In Equation (4), η_∞ is the high-temperature limit of viscosity, and W_1, C_1, W_2 and C_2 are adjustable parameters. The fitted parameter values for the blue line are: $\log \eta_\infty = -2.95 \pm 0.04$, $W_1 = 5.3 \pm 2.2\ \mathrm{K}^{-1}$, $C_1 = 5334 \pm 231$ K, $W_2 = (5.79 \pm 0.71) \times 10^{-4}\ \mathrm{K}^{-1}$ and C_2 459±45 K, with the quality of fit given by $R^2 = 0.9997$. Given the lack of data, particularly at high temperatures near to T_m, this line must be regarded as only an approximate description of $\eta(T)$ for AIST.

Using Equations (5) and (6) as detailed above, and taking a representative temperature of $500\,\mathrm{K}$, we have $U_{\mathrm{kin}}\left(\mathrm{m\,s^{-1}}\right) = \left(8.1 \times 10^{-3}\right) / \eta(\mathrm{Pa\,s})$. Salinga et al.[15] followed essentially the same analysis, but took different values for the characteristic length scales (atomic radius, diffusional jump distance, hydrodynamic radius). With their values, $U_{\mathrm{kin}}\left(\mathrm{m\,s^{-1}}\right) = \left(8.8 \times 10^{-1}\right) / \eta(\mathrm{Pa\,s})$. Thus the corresponding values of $U(T)$ and $\eta(T)$ in the present work and in Salinga et al. are different. The comparison of different of $\eta(T)$ values, for example in Figure 3, is affected as some are directly from viscosity measurements, others inferred from growth rates.

The low-temperature data for $Te_{85}Ge_{15}$ shown in Figure 3 were derived from crystallization kinetics, and they correspond to a fragility of $m \approx 25$. Alternatively, the fragility can be estimated using $m = Q(T_g) / \left(\ln 10 R T_g\right)$, where $Q(T_g)$ is an effective activation energy obtained from the shift of T_g with heating rate Φ in the DSC data in Ref. [26]. In this way the fragility is estimated to be 30–40, depending on exactly how $Q(T_g)$ is determined.

This approximate value for *m*, similar to that for AIST at low temperature, is so low that it is impossible to fit to the high-temperature data of Neumann et al.[25] Thus there is still a clear, though less pronounced, fragile-to-strong crossover.

Acknowledgements

C. E. Smith and Mettler-Toledo are thanked for access to the ultrafast DSC facilities. B. Gholipour is thanked for assistance with thin-film deposition. J.O., D.W.H. and A.L.G. acknowledge support from the Engineering and Physical Sciences Research Council (EPSRC, UK), D.W.H. in part through the EPSRC Centre for Innovative Manufacturing in Photonics. J.O. and A.L.G. acknowledge support from the World Premier International Research Center Initiative (WPI), MEXT, Japan. C. A. Angell, L. Battezzati, G. Dalla Fontana and M. Salinga are thanked for helpful discussions.

Received: (will be filled in by the editorial staff)
Revised: (will be filled in by the editorial staff)
Published online: (will be filled in by the editorial staff)

[1] S. Raoux, W. Welnic, D. Ielmini, *Chem. Rev.* **2010**, *110*, 240.

[2] a) C. D. Wright, P. Hosseini, J. A. Vazquez Diosdado, *Adv. Funct. Mater.* **2013**, *23*, 2248; b) D. Kuzum, S. Yu, H.-S. P. Wong, *Nanotechnol.* **2013**, *24*, 382001.

[3] W. Wang, D. Loke, L. Shi, R. Zhao, H. Yang, L.-T. Law, L.-T. Ng, K.-G. Lim, Y.-C. Yeo, T.-C. Chong, A. L. Lacaita, *Sci. Rep.* **2012**, *2*, 360.

[4] M. Wuttig, M. Salinga, *Nat. Mater.* **2012**, *11*, 270.

[5] G. F. Zhou, *Mater. Sci. Eng. A* **2001**, *304–306*, 73.

[6] J. Kalb, F. Spaepen, M. Wuttig, *Appl. Phys. Lett.* **2004**, *84*, 5240.

[7] J. Orava, A. L. Greer, B. Gholipour, D. W. Hewak, C. E. Smith, *Nat. Mater.* **2012**, *11*, 279.

[8] C. A. Angell, *Science* **1995**, *267*, 1924.

[9] G. W. Burr, P. Tchoulfian, T. Topuria, C. Nyffeler, K. Virwani, A. Padilla, R. M. Shelby, M. Eskandari, B. Jackson, B.-S. Lee, *J. Appl. Phys.* **2012**, *111*, 104308.

[10] A. Sebastian, M. Le Gallo, D. Krebs, *Nat. Commun.* **2014**, *5*, 4314.

[11] R. Jeyasingh, S. W. Fong, J. Lee, Z. Li, K.-W. Chang, D. Mantegazza, M. Asheghi, K. E. Goodson, H.-S. P. Wong, *Nano Lett.* **2014**, *14*, 3419.

[12] N. Ciocchini, M. Cassinerio, D. Fugazza, D. Ielmini, *IEEE Trans. Electron Devices* **2013**, *60*, 3767.

[13] M. D. Ediger, P. Harrowell, L. Yu, *J. Chem. Phys.* **2008**, *128*, 034709.

[14] G. C. Sosso, J. Behler, M. Bernasconi, *Phys. Status Solidi B* **2012**, *249*, 1880.

[15] M. Salinga, E. Carria, A. Kaldenbach, M. Bornhöfft, J. Benke, J. Mayer, M. Wuttig, *Nat. Commun.* **2013**, *4*, 2371.

[16] J. Orava, A. L. Greer, *Thermochim. Acta* **2015**, *603*, 63.

[17] W. K. Njoroge, H. Dieker, M. Wuttig, *J. Appl. Phys.* **2004**, *96*, 2624.

[18] J. Orava, A. L. Greer, B. Gholipour, D. W. Hewak, C. E. Smith, *Appl. Phys. Lett.* **2012**, *101*, 091906.

[19] J. Kalb, F. Spaepen, M. Wuttig, *J. Appl. Phys.* **2003**, *93*, 2389.

[20] M. H. Cohen, G. S. Grest, *Phys. Rev. B* **1979**, *20*, 1077.

[21] C. V. Thompson, F. Spaepen, *Acta Metall.* **1979**, *27*, 1855.

[22] J. Kalb, F. Spaepen, T. P. Leervad Pedersen, M. Wuttig, *J. Appl. Phys.* **2003**, *94*, 4908.

[23] C. Zhang, L. Hu, Y. Yue, J. C. Mauro, *J. Chem. Phys.* **2010**, *133*, 014508.

[24] J. Akola, R. O. Jones, *Appl. Phys. Lett.* **2009**, *94*, 251905.

[25] H. Neumann, F. Herwig, W. Hoyer, *J. Non. Cryst. Solids* **1996**, *205–207*, 438.

[26] J. Rocca, M. Erazú, M. Fontana, B. Arcondo, *J. Non. Cryst. Solids* **2009**, *355*, 2068.

[27] S. Stølen, T. Grande, H.-B. Johnsen, *Phys. Chem. Chem. Phys.* **2002**, *4*, 3396.

[28] Y. Gueguen, T. Rouxel, P. Gadaud, C. Bernard, V. Keryvin, J.-C. Sangleboeuf, *Phys. Rev. B* **2011**, *84*, 064201.

[29] J. A. Kalb, M. Wuttig, F, Spaepen, *J. Mater. Res.* **2007**, *22*, 748.

[30] W. Zhang, I. Ronneberger, P. Zalden, M. Xu, M. Salinga, M. Wuttig, R. Mazzarello, *Sci. Rep.* **2014**, *4*, 6529.

[31] C. A. Angell, *J. Phys. Chem.* **1993**, *97*, 6339.

[32] I. Saika-Voivod, P. H. Poole, F. Sciortino, *Nature* **2001**, *412*, 514.

[33] Y. Tsuchiya, *J. Non. Cryst. Solids* **1993**, *156–158*, 704.

[34] L. Battezzati, A. L. Greer, *J. Mater. Res.* **1988**, *3*, 570.

[35] C.-Z. Zhang, L.-N. Hu, X.-F. Bian, Y.-Z. Yue, *Chin. Phys. Lett.* **2010**, *27*, 116401.

[36] C. Zhou, L. Hu, Q. Sun, H. Zheng, C. Zhang, Y. Yue, *J. Chem. Phys.* **2015**, *142*, 064508.

[37] M. C. Wilding, M. Wilson, P. F. McMillan, *Chem. Soc. Rev.* **2006**, *35*, 964.

[38] B. Kalkan, S. Sen, J.-Y. Cho, Y.-C. Joo, S. M. Clark, *Appl. Phys. Lett.* **2012**, *101*, 151906.

[39] M. Kalyva, J. Orava, A. Siokou, M. Pavlista, T. Wagner, S. N. Yannopoulos, *Adv. Funct. Mater.* **2013**, *23*, 2052.

[40] C. Way, P. Wadhwa, R. Busch, *Acta Mater.* **2007**, *55*, 2977.

[41] H.-L. Luo, *PhD Thesis*, California Institute of Technology, **1964**.

[42] J. Orava, A. L. Greer, *J. Chem. Phys.* **2014**, *140*, 214504.

[43] K. F. Kelton, A. L. Greer, *Nucleation in Condensed Matter: Applications in Materials and Biology*, Elsevier, Pergamon Materials Series, Oxford, UK **2010**, p. 498.

[44] A. L. Greer, *Mater. Sci. Eng. A* **1991**, *133*, 16.

[45] G. Eising, T. van Damme, B. J. Kooi, *Cryst. Growth Des.* **2014**, *14*, 3392.

[46] B.-S. Lee, R. M. Shelby, S. Raoux, C. T. Retter, G. W. Burr, S. N. Bogle, K. Darmawikarta, S. G. Bishop, J. R. Abelson, *J. Appl. Phys.* **2014**, *115*, 063506.

[47] F. Mallamace, C. Branca, C. Corsaro, N. Leone, J. Spooren, S.-H. Chen, H. E. Stanley, *Proc. Nat. Acad. Sci.* **2010**, *107*, 22457.

[48] J.-Y. Cho, D. Kim, Y.-J. Park, T.-Y. Yang, Y.-Y. Lee, Y.-C. Joo, *Acta Mater.* **2015** *94*, 143.

[49] a) E. Zhuravlev, C. Schick, *Thermochim. Acta* **2010**, *505*, 1; b) E. Zhuravlev, C. Schick, *Thermochim. Acta* **2010**, *505*, 14.

[50] J. C. Mauro, Y. Yue, A. J. Ellison, P. K. Gupta, D. C. Allan, *Proc. Nat. Acad. Sci.* **2009**, *106*, 19780.

[51] G. Adam, J. H. Gibbs, *J. Chem. Phys.* **1965**, *43*, 139.

The *Table of Contents* entry:

The temperature-dependent viscosity inferred for liquid Ag-In-Sb-Te (AIST) presents evidence for a *fragile-to-strong crossover* on cooling the liquid. Such a crossover is relevant for the application of AIST and other chalcogenides, helping to understand the distinction between nucleation- and growth-dominated crystallization, and guiding materials design to combine fast switching and non-volatility for application in phase-change memory and neuromorphic computing.

ToC figure